THE JOURNAL OF PHYSICAL CHEMISTRY C
A JOURNAL OF THE AMERICAN CHEMICAL SOCIETY

pubs.acs.org/JPCC Article

Enhancing the Photoluminescence and Stability of Methylammonium Lead Halide Perovskite Nanocrystals with Phenylalanine

Li Liu, Ke Xu, A' Lester Allen, Xueming Li, Hong Xia, Lijun Peng, and Jin Z. Zhang*

Cite This: *J. Phys. Chem. C* 2021, 125, 2793−2801 Read Online

ACCESS | Metrics & More | Article Recommendations | Supporting Information

ABSTRACT: The choice of ligand is an important parameter in the synthesis of metal halide perovskites such as methylammonium lead bromide ($MAPbBr_3$) perovskite nanocrystals (PNCs). In this work, phenylalanine (Phe) was demonstrated, for the first time, as a highly effective capping ligand for synthesizing $MAPbBr_3$ PNCs when used in conjunction with (3-aminopropyl) triethoxysilane (APTES) and oleic acid (OA) or methylphosphoric acid (MPA). Ultraviolet−visible absorption and photoluminescence (PL) emission spectroscopy, powder X-ray diffraction, and Fourier transform infrared spectroscopy were used to investigate the optoelectronic, structural, and surface properties of the PNCs. The combined use of Phe, APTES, and OA or MPA is demonstrated to be highly successful in passivating PNCs for achieving both improved PL and enhanced stability. The enhanced passivation by Phe is attributed to the three functional groups in Phe that can stabilize surface defects related to Pb^{2+}, $CH_3NH_3^+$, and Br^- by mediating pH and hydrophobicity. Based on all the experimental results, a model is proposed to explain the passivation mechanism involving Phe in conjunction with other amine and acid ligands. This study demonstrates the effectiveness of multiligand passivation of perovskites involving amino acid as the capping ligand.

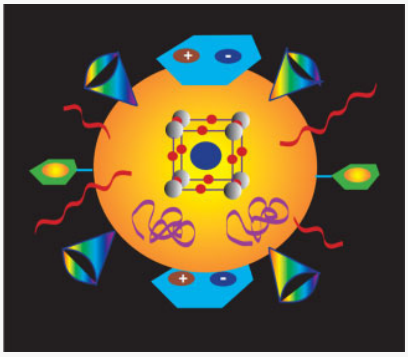

Downloaded via UNIV OF CALIFORNIA SANTA CRUZ on May 16, 2021 at 18:20:40 (UTC).
See https://pubs.acs.org/sharingguidelines for options on how to legitimately share published articles.

INTRODUCTION

Organo-metal halide perovskites, such as methylammonium lead halide ($MAPbX_3$, with MA = $CH_3NH_3^+$ and X = Cl^-, Br^-, I^-), have attracted significant attention due to their intriguing optoelectronic properties.[1,2] Perovskite nanocrystals (PNCs) or quantum dots afford the additional advantage of size-tunable optical properties desired for many applications.[3−5] However, surface defects of PNCs due to dangling bonds make them susceptible to degradation and long-term instability, which is a major impediment toward their processability and applications.[6,7] Many efforts have been devoted to developing synthesis strategies to produce high-quality PNCs with good stability and desired optical properties.[3,8−12] One major culprit for the fast degradation of PNCs is the labile surface capping.[11,13,14] Appropriate capping ligands on the surface of PNCs not only reduce surface defects and related trap states but can also prevent molecules such as water and oxygen from reaching the PNC surface to cause degradation.[15−18]

To date, organic acids and organic bases such as amines have been commonly used as ligands in the synthesis of PNCs.[19−22] The carboxylates presumably chelate with surface lead atoms, while alkylammonium interacts with the surface via hydrogen bonding ($X^-\cdots H-N$) or ionic bonding ($X^-\cdots NH_3^+$).[23] However, the prepared PNCs could lose surface ligands during purification.[24,25] Compared to ligands with a straight chain, branched capping ligands improve the stability of PNCs due to strong steric effects. For example, Luo et al. produced size-tunable $MAPbBr_3$ PNCs, with much better stability against a protonic solvent, by employing (3-aminopropyl) triethoxysilane (APTES) and polyhedral oligomeric silsesquioxane (POSS) PSS-[3-(2-aminoethyl) amino] propylheptaisobutyl-substituted (NH_2-POSS).[26] In this case, APTES was chosen as both a capping ligand and precursor for a thin layer of silica on the PNC surface that further protects the PNCs from species such as water, oxygen, or other protonic solvent molecules.

Different passivation strategies have been developed to improve the stability of PNCs via ligand engineering, taking advantage of different interactions between the ligand and surface defects including hydrogen-bonding and electrostatic interactions.[10,27−32] A combination of organic amines and acids has been found to be particularly powerful for passivating PNCs as proton transfer between the amines and acids results in ammonium and carboxylate ions that are effective or stabilizing charged surface defects.[33] Amino acids and peptide-like molecules with both amine and acid functional groups

Received: December 12, 2020
Revised: January 8, 2021
Published: January 21, 2021

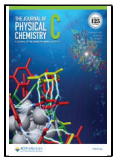

ACS Publications © 2021 American Chemical Society

https://dx.doi.org/10.1021/acs.jpcc.0c11095
J. Phys. Chem. C 2021, 125, 2793−2801

afford some unique features as multidentate ligands for passivating PNCs, targeting defects such as $CH_3NH_3^+$, Pb^{2+}, and X^-.[34−36] For example, bidentate peptide-like ligands, such as 12-aminododecanoic acid, were found to be effective in passivating $MAPbBr_3$ PNCs.[37] Likewise, proteinogenic essential amino acids, L-Lysine (LYS) and *L*-Arginine (ARG), have been used for surface passivation of $MAPbBr_3$ PNCs.[38] Similarly, leucine was used in the synthesis of $MAPbBr_3$ PNCs,[39] *L*-alanine (LA) was found to enhance charge transfer between perovskite and TiO_2,[40] and *L*-cysteine (*L*-cys) was used in controllable synthesis of $MAPbBr_3$ PNCs.[41] These studies show that amino acids are promising ligands for passivating PNCs to improve their properties for emerging applications.[42−44]

Recently, a "cocktail" approach involving the use of a combination of ligands has been suggested for effective passivation of different surface defects.[33] For metal halide perovskites, the multiple and varied defects expected require several different ligands for optimal passivation. Theoretical simulations also reveal that there are different types of defects on the surface of perovskites, which require the corresponding ligands to passivate.[45]

In this work, we introduce proteinogenic essential amino acid phenylalanine (Phe) with APTES and oleic acid (OA) or methylphosphoric acid (MPA) as multicapping ligands for PNC synthesis. Phe was found to enhance photoluminescence (PL) quantum yield (QY) and improve the stability of the PNCs. Fourier transform infrared (FTIR) study reveals that the charged ammonium and carboxylate or phosphate groups are effective in synergistically passivating Br^-, Pb^{2+}, and $CH_3NH_3^+$ defects on the surface of PNCs. We also found that the use of different acid ligands affects the way Phe exists and how it is involved in the passivation of surface defects. A model is proposed to explain the passivation mechanism based on specific pair-wise interactions between ligands and defects.

METHODS

Materials. Methylammonium bromide (CH_3NH_3Br, 99.9%, Greatcell Solar), lead bromide ($PbBr_2$, 99.999%, Alfa Aesar), oleic acid (OA, 90%, Sigma Aldrich), methylphosphoric acid (MPA, 98%, Fluka), *N*,*N*-dimethylformamide (DMF, 99.9%, Fisher Scientific), (3-aminopropyl) triethoxysilane (APTES, 99%, Sigma-Aldrich), toluene (99.9%, Fisher Scientific), aspartic acid (Asp), *L*-asparagine (Asn), phenylalanine (Phe), and isopropanol (99.999%, Alfa Aesar) were commercially available. All chemicals were used as received without any further purification.

Synthesis of OA-APTES-Phe-$MAPbBr_3$ PNCs. The precursor solution of OA-APTES-Phe-$MAPbBr_3$ was prepared by dissolving 0.080 mmol CH_3NH_3Br, 0.20 mmol $PbBr_2$, 0.32 mmol OA, 0.085 mmol APTES, and 0.050 mmol Phe in 0.40 mL of DMF solvent, and then, the solution was sonicated for 30 min and heated at 70 °C until it became transparent. The precursor solution was then quickly injected into 5.0 mL of toluene. The precipitate was washed with toluene three times and collected by centrifugation and then dried in a vacuum overnight. The molar ratio between $PbBr_2$ and CH_3NH_3Br is known to affect the generated PNCs, with a ratio of higher than 1 producing PNCs with a higher PL QY,[9,26,31,37] possibly due to excess Pb^{2+} ions leading to better surface passivation. Therefore, we used a fixed CH_3NH_3Br (0.080 mmol) and $PbBr_2$ (0.20 mmol) to prepare the PNCs.

Synthesis of MPA-APTES-Phe-$MAPbBr_3$ PNCs. The precursor solution of MPA-APTES-Phe-$MAPbBr_3$ was prepared by dissolving 0.080 mmol CH_3NH_3Br, 0.20 mmol $PbBr_2$, 0.050 mmol MPA, 0.085 mmol APTES, and 0.050 mmol Phe in 0.40 mL of DMF solvent, and then, the solution was sonicated for 30 min and heated at 70 °C until it became transparent. The precursor solution was then quickly injected into 5.0 mL of toluene, resulting in PNCs as a precipitate. The precipitate was washed with toluene three times, collected by centrifugation, and then dried in a vacuum overnight. Other syntheses reported in this study were carried out using similar reactions as above at a fixed precursor concentration and different types of amino acids.

Stability Test of $MAPbBr_3$ PNCs. A total of 0.50 mg/mL of $MAPbBr_3$ PNC precipitate was dispersed in isopropanol and sonicated for 10 min. The PL intensity of the samples was tested every half hour. The stability study also carried out in isopropanol under UV continuous excitation for 1 hour.

PL QY Measurement. The PL QY of $MAPbBr_3$ PNCs was calculated by utilizing the following equation.

$$\mathrm{PLQY} = \mathrm{PLQY}_{\mathrm{st}} \frac{F_{\mathrm{st}}}{F_x} \frac{A_x}{A_{\mathrm{st}}}$$

where the subscript *x* and *st* represent the sample and standard, respectively. Rhodamine 6G (95% PL QY) is used as the standard. *F* is the integrated PL intensity, and *A* is the absorbance.

Characterizations. Ultraviolet−visible (UV−vis) absorption spectra were measured with an Agilent Technologies Cary 60 UV−vis spectrophotometer, and the PL spectra were measured using a HORIBA Jobin Yvon Fluoromax-3 spectrofluorometer using a quartz cuvette (1.0 cm × 1.0 cm) at room temperature. Transmission electron microscopy (TEM) was performed using an FEI UT Tecnai microscope operated at 200 kV acceleration voltage at the National Center for Electron Microscopy in Lawrence Berkeley National Laboratory. X-ray diffraction (XRD) data were acquired using a Rigaku American Miniflex Plus power diffractometer at a voltage of 40 kV and current of 30 mA, with a scanning angle of 10−70 (2θ) and rate of 3° min^{-1}. FTIR spectra were obtained with a PerkinElmer FTIR spectrometer (Spectrum One, spectral resolution 4 cm^{-1}), where the samples were prepared by dropping the $MAPbBr_3$ PNC solution onto a KBr pellet.

RESULTS AND DISCUSSION

Optical Properties of $MAPbBr_3$ PNCs. Different amino acids, such as Phe, Asp, and Asn, were used to synthesize $MAPbBr_3$ PNCs in order to gain insight into how they may affect the properties of the resulting PNCs. The chemical structures of the three amino acids are showed in Figure 1A. The UV−vis absorption and PL spectra of OA-APTES-$MAPbBr_3$ PNCs (labeled as OAA-PNCs) are shown in Figure 1B,C. Interestingly, although the solubility of Asn and Asp is less than that of Phe in DMF used as the solvent for the synthesis, they all show enhanced PL. Meanwhile, with the introduction of Phe (labeled as OAA-Phe-PNCs), Asp (labeled as OAA-Asp-PNCs), and Asn (labeled as OAA-Asn-PNCs), both the excitonic absorption peak and PL peak show a slight red-shift, likely due to a small increase in the size of the PNCs. The OAA-Phe-PNCs have the highest PL intensity, indicating that Phe provided the best surface passivation. This may be

https://dx.doi.org/10.1021/acs.jpcc.0c11095
J. Phys. Chem. C 2021, 125, 2793−2801

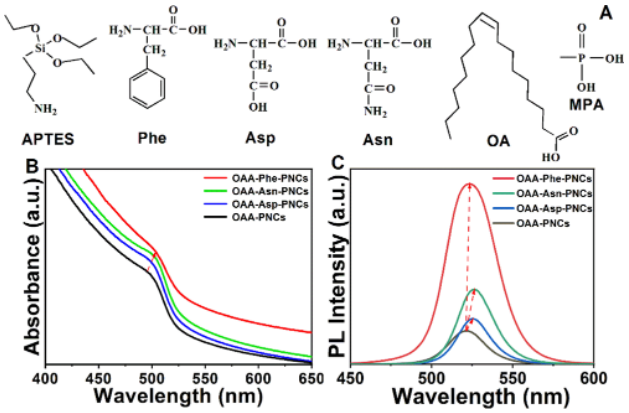

Figure 1. (A) Molecular structures of APTES, Phe, Asp, Asn, OA, and MPA; (B) UV−vis absorption and (C) PL spectra of OAA-PNCs, OAA-Phe-PNCs, OAA-Asn-PNCs, and OAA-Asp-PNCs.

related to the unique molecular structure of Phe compared with Asp and Asn in which the presence of the benzene ring may help passivation, as explained in more detail later.[8,46,47]

In order to better understand the role of Phe, a series of control experiments have been conducted on APTES-Phe-$MAPbBr_3$ PNCs, OAA-PNCs, and OAA-Phe-PNCs. The UV−vis absorption and PL spectra are shown in Figure 2. APTES-Phe-$MAPbBr_3$ PNCs have an absorption band centered at 496 nm and PL peak at 515 nm with a full width half maximum (FWHM) of ∼55 nm, while OAA-PNCs have an absorption peak at 493 nm and PL peak at 513 nm with a FWHM of ∼32 nm. The electronic absorption spectra of APTES-Phe-$MAPbBr_3$ PNCs and OAA-PNCs have some "tail" absorption at wavelength longer than that of the excitonic absorption peak, which may be due to some aggregates in solution that scatter light. For APTES-Phe-$MAPbBr_3$ PNCs, the broad FWHM is likely related to broader size distribution of the PNCs. The PL QY values were calculated to be 56 and 44% for APTES-Phe-$MAPbBr_3$ and OAA-PNCs, respectively. Meanwhile, OAA-Phe-PNCs exhibited a strong absorption peak at 501 nm and PL peak at 517 nm. The emission peak becomes narrower with the FWHM decreased to ∼27 nm, and the PL QY value was up to 78%. Complete optical data are summarized in Supporting Information Table S1. We suggest that the difference in PL QY is due to the density of trap states of the PNCs that strongly depends on the effectiveness of passivation by the ligands. The observed red-shift in absorption and PL is likely due to an increase in PNC size. Well-passivated PNCs with the highest PL QY were obtained when OA, APTES, and Phe were used, indicating the synergistic effect among the three capping ligands.

Similar PL enhancement was also observed in MPA-APTES-$MAPbBr_3$ PNCs (labeled as MPAA-PNCs) as shown in Figure 3A. After the introduction of Phe (labeled as MPAA-Phe-PNCs), Asp (labeled as MPAA-Asp-PNCs), and Asn (labeled as MPAA-Asn-PNCs), the PL intensity of the PNCs increased, and the PL peak was slightly red-shifted. The PL QY of MPAA-Phe-PNCs and MPAA-PNCs was measured to better understand the increased passivation efficiency. As shown in Table S1, the PL QY of the prepared PNCs increased from 77 to 87% with the introduction of Phe. The FWHM of the ensemble spectra of MPAA-Phe-PNCs is typically ∼5 nm narrower than that of MPAA-PNCs (Figure 3B,C), which indicates a narrow size distribution of MPAA-Phe-PNCs.

Structural Characterization of $MAPbBr_3$ PNCs. The morphology of OAA-Phe-PNCs was analyzed by TEM. As shown in Figure S1 in the Supporting Information, the average diameter of the OAA-Phe-PNCs is 10.2 ± 1.7 nm. The particles tend to aggregate, similar to what was reported in previous work.[26,48,49] When APTES is used as the capping ligand in the synthesis of PNCs, its hydrolysis with a small amount of water in air leads to the formation of a very thin SiO_2 layer on the surface of the PNCs. The presence of SiO_2 seems to cause some aggregation even in solution. In addition, the toluene solvent evaporated to produce a supersaturated solution when making TEM grids, and this also caused the PNCs to aggregate during the drying process.[50]

Figure 4 shows the XRD patterns of the $MAPbBr_3$ PNCs with Phe, Asp, and Asn as additional passivating ligands (in addition to OA or MPA and APTES) and the XRD patterns of PNCs without the amino acids shown for comparison. Peaks at 14.85, 21.11, 30.06, 33.65, 37.04, 43.07, and 45.81° correspond to the reflections (001), (011), (002), (021), (211), (220), and (300) of $MAPbBr_3$, respectively, indicating the cubic structure.[31,38,51,52] The same peaks were observed for the amino acid-based PNCs, indicating that the amino acids do not affect the crystal structure of the perovskite core.

Figure 5 shows the FTIR spectra of OAA-PNCs, OAA-Phe-PNCs, OAA-Asn-PNCs, and OAA-Asp-PNCs. For all the samples, the characteristic bands at 2850 and 2920 cm^{-1} are assigned to the symmetric and asymmetric C−H stretch mode.[31,37] The bands at 1466 and 1568 cm^{-1} correspond to the symmetric and asymmetric stretch vibrations of the $-COO^-$ group,[53] and the band at 1710 cm^{-1} is assigned to the stretch vibration of C═O,[37,54] confirming the presence of OA as the capping ligand on the PNC surface. The band at 910 cm^{-1} is assigned to the Si−OH stretch vibration, the band at 1020 cm^{-1} originated from the stretch vibration of Si−O−C, and the band at 1110 cm^{-1} can be ascribed to the stretch vibration of Si−O−Si.[31] The band at 1213 cm^{-1} can be assigned to the stretch vibration of C−N. The characteristic

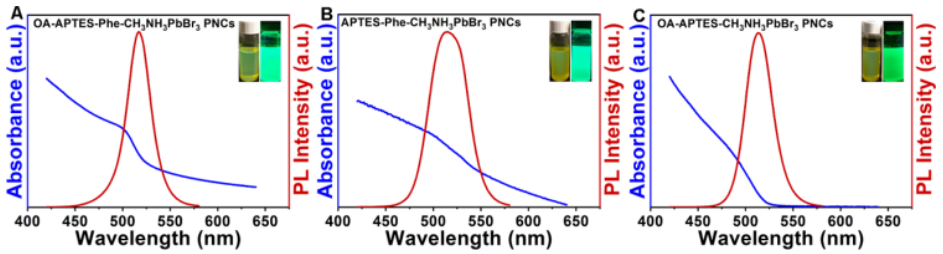

Figure 2. UV−vis absorption and PL spectra of (A) OAA-Phe-PNCs, (B) APTES-Phe-$MAPbBr_3$ PNCs, and (C) OAA-PNCs. Insets show digital photographs of the respective PNC solution under natural light and irradiation with UV light.

https://dx.doi.org/10.1021/acs.jpcc.0c11095
J. Phys. Chem. C 2021, 125, 2793−2801

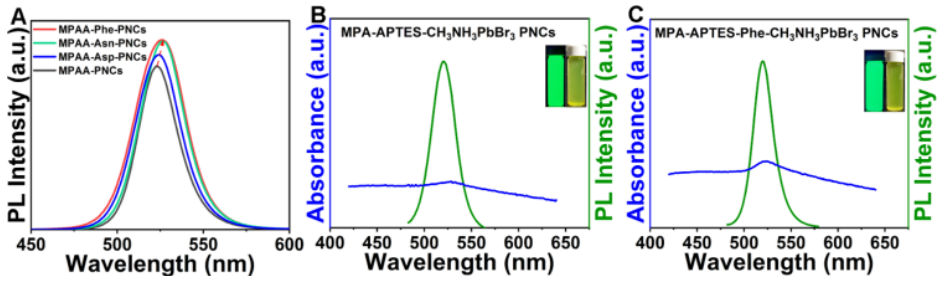

Figure 3. (A) PL spectra of MPAA-PNCs, MPAA-Phe-PNCs, MPAA-Asn-PNCs, and MPAA-Asp-PNCs; UV−vis absorption and PL spectra of (B) MPAA-PNCs and (C) MPAA-Phe-PNCs. Insets show digital photographs of the respective PNC solution under natural light and irradiation with UV light.

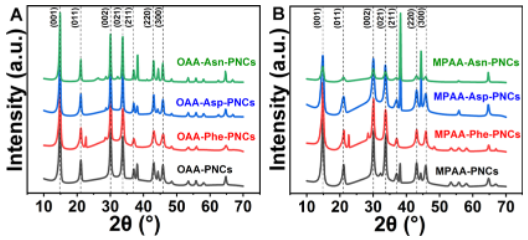

Figure 4. XRD patterns of (A) OAA-PNCs with and without amino acids and (B) MPAA-PNCs with and without amino acids. Different amino acids were studied, such as Phe, Asp, and Asn.

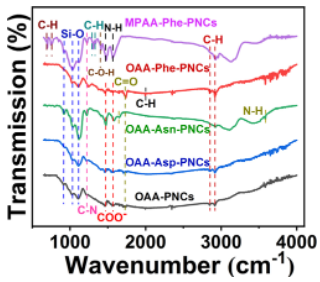

Figure 5. FTIR spectra of OAA-PNCs, OAA-Asp-PNCs, OAA-Asn-PNCs, OAA-Phe-PNCs, and MPAA-Phe-PNCs.

band of Si−OH demonstrates that the hydrolysis condensation of APTES occurred, while the band of Si−O−Si confirmed that a wrapped silica layer was formed on the PNC surface.[48] For OAA-Asn-PNCs, there are two peaks at 1645 and 3586 cm^{-1} corresponding to the stretch vibration of C═O and N−H for primary amide, indicating the existence of Asn. For OAA-Phe-PNCs, there is a weak peak at around 2000 cm^{-1} corresponding to the bending mode of CH_2 of the aromatic compound, indicating the existence of Phe.

FTIR for MPAA-Phe-PNCs was also performed. As shown in Figure 5, there are two sharp peaks at 697 and 750 cm^{-1} corresponding to the vibration frequencies of the external plane of the $-CH_2$ aromatic ring.[9,54] The peaks in the range of 1087 to 1335 cm^{-1} attributed to the three differently protonated states of methylphosphonic acid, in conjunction with literature data on frequency values for $-CH_3$ and P−C groups.[55] The bands at 1482 and 1580 cm^{-1} correspond to the symmetric and asymmetric deformation vibrations of the $-NH_3^+$ group.[56] The band around the 1400 cm^{-1} wavenumber region is assigned to the in-plane bending mode of C−O−H.[35] The band assignments are summarized in Table S2. The FTIR results indicate that OA molecules are bound to the surface of PNCs by the $-COO^-$ group, while MPA molecules are bound by the $-PO_3^{2-}$ and $-PO_3H^-$ groups. The results also indicate a silica layer on the surface of PNCs due to hydrolyzed APTES as well as the presence of amino acids.

Improvement of the Chemical Stability of $MAPbBr_3$ PNCs. The stability of the PNCs was studied at room temperature by measuring relative PL intensity for 2.0 h in ambient air and isopropanol solvent. As shown in Figure 6A,

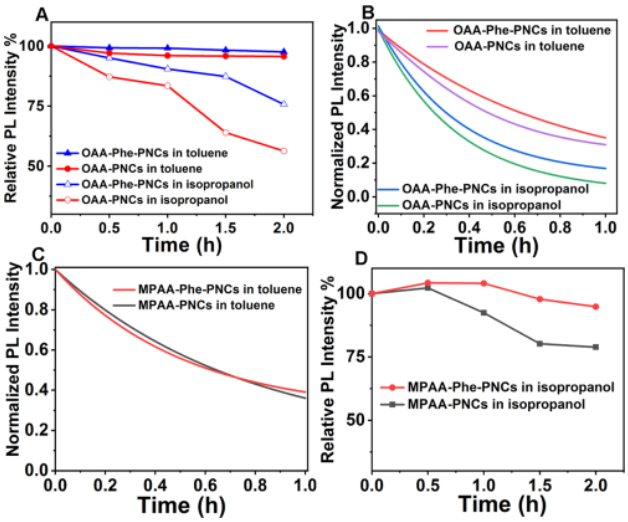

Figure 6. (A) Relative PL intensity of 0.50 mg/mL for OAA-PNCs and OAA-Phe-PNCs in toluene and isopropanol in the dark for different times; (B) normalized PL intensity of OAA-PNC and OAA-Phe-PNC solution as a function of the illumination time; (C) normalized PL intensity of MPAA-PNCs and MPAA-Phe-PNCs in toluene solution as a function of the illumination time; (D) relative PL intensity of 0.50 mg/mL of MPAA-PNCs and MPAA-Phe-PNCs in isopropanol in the dark for different times. The sample was continuously irradiated using a fluorimeter excitation lamp (λ_{exc} = 365 nm).

when the PNCs were dispersed in toluene in ambient air and in the dark, the relative PL intensity of OAA-PNCs and OAA-Phe-PNCs was 95 and 98% after 2.0 h, respectively. While the relative PL intensity of the OAA-Phe-PNC precipitate in isopropanol remained almost 76%, only 56% remained for OAA-PNCs. A stability test was also carried out by measuring PL intensity for 1.0 h in ambient air and under continuous irradiation with a fluorimeter excitation lamp (λ_{exc} = 365 nm). The normalized PL intensity of OAA-Phe-PNCs and OAA-PNCs in toluene remained more than 30% after 1.0 h, whereas that of PNCs in isopropanol decreased less than 20% (Figure 6B). Detailed stability data are summarized in Table S3. The

https://dx.doi.org/10.1021/acs.jpcc.0c11095
J. Phys. Chem. C 2021, 125, 2793−2801

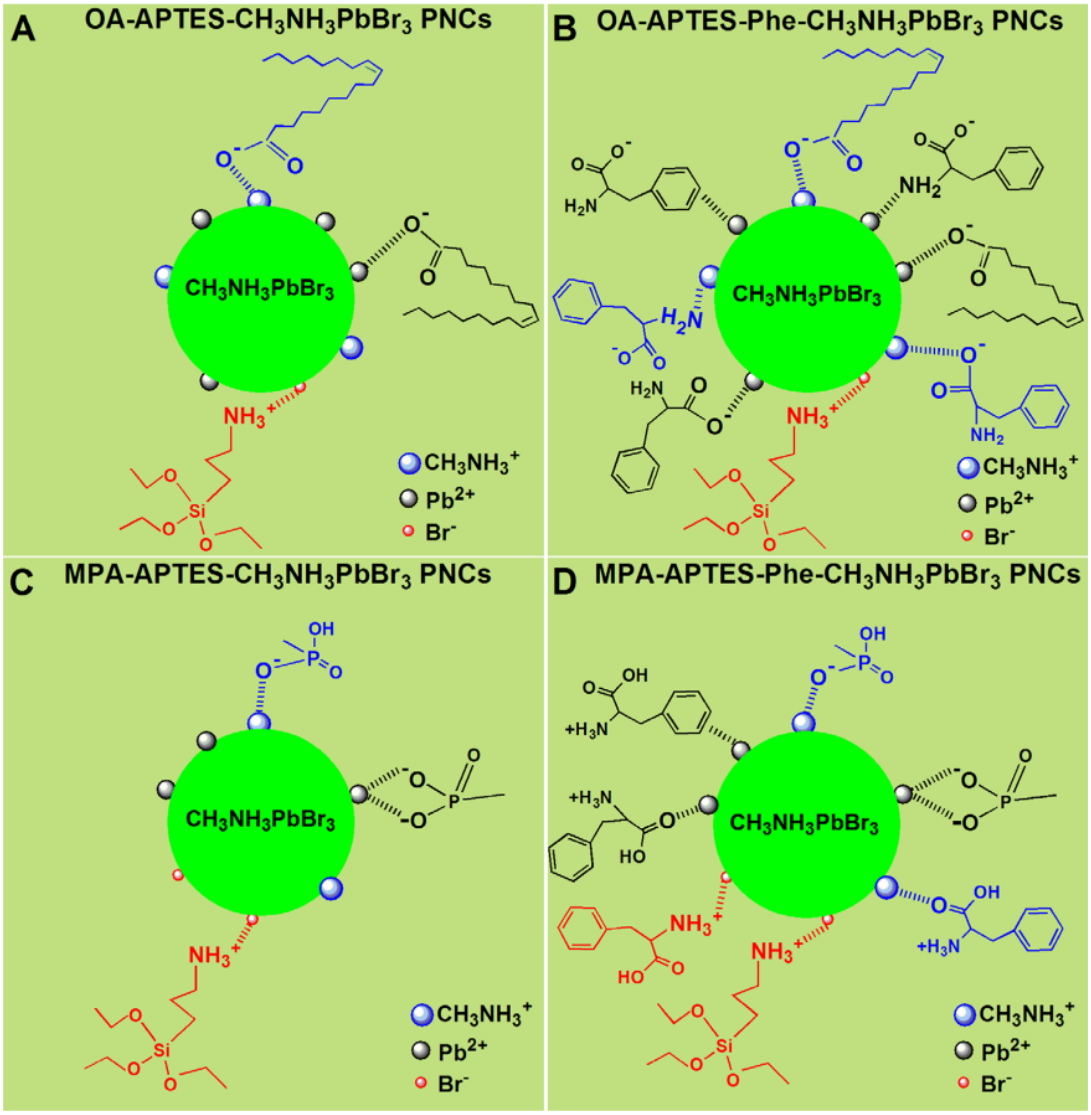

Figure 7. Ligand binding modes on the surface of four PNC samples: (A) OAA-PNCs, (B) OAA-Phe-PNCs, (C) MPAA-PNCs, and (D) MPAA-Phe-PNCs.

degradation in the dark is mainly attributed to the reaction with oxygen molecules in air or protonic solvent molecules, while with light, the degradation is likely caused by superoxide produced by light and oxygen.[57,58] The improved stability by Phe could partly be due to the hydrophobic benzene ring that can prevent water or oxygen molecules from reaching the perovskite core.

The stability of MPAA-PNCs and MPAA-Phe-PNCs was also evaluated by measuring normalized PL intensity for 1 h under 365 nm UV continuous illumination in toluene. As shown in Figure 6C, the normalized PL intensity for MPAA-PNCs and MPAA-Phe-PNCs decreased to 33 and 35%, respectively. The relative PL intensity of MPAA-PNCs and MPAA-Phe-PNCs in the isopropanol solvent remained 79 and 95% after 2.0 h, respectively (Figure 6D). Detailed stability data are summarized in Table S3. The degradation mechanisms should be similar to those of OAA-based PNCs.

While APTES and OA or MPA stabilized $MAPbBr_3$ PNCs are stable in toluene, they are not stable under continuous illumination in ambient air, especially when immersed in polar solvent such as isopropanol. The introduction of Phe enhanced the stability of PNCs in polar solvent. If Phe is used in conjunction with APTES and OA (or MPA), the resulting PNCs have higher PL stability than those without Phe. This is possibly because Phe helps to prevent oxygen or protonic solvent molecules from reaching the PNC core, especially through the hydrophobic benzene ring.

Mechanism of Surface Passivation. The ionic character and ternary nature of metal halide perovskites are expected to lead to multiple ionic defects in $MAPbBr_3$ PNCs that are related to $CH_3NH_3^+$, Pb^{2+}, and Br^-. Passivation of the surface defects with ligands is critical to their properties and functionality including stability. FTIR analyses suggest the presence of C═O, $-COO^-$, $-PO_3^{2-}$, $-PO_3H^-$, −Si−O, and $-C_6H_5$ on the surface of the PNCs studied, which indicate successful passivation of the PNCs by OA or MPA, APTES, and Phe ligands.

In the OAA-PNC system, OA and APTES are used in conjunction, and the reaction between OA and APTES can be described using the corresponding acid dissociation constants

https://dx.doi.org/10.1021/acs.jpcc.0c11095
J. Phys. Chem. C 2021, 125, 2793−2801

K_a and base dissociation constant K_b (see the Supporting Information). OA could react with APTES to generate octylammonium and oleate via proton transfer, and the oleate can use its carboxylate group to chelate with the surface $CH_3NH_3^+$ and Pb^{2+}, while the ammonium group in octylammonium can bind to surface Br^-. Additionally, during the synthesis process, the system was exposed to air and a trace amount of water can react with APTES via hydrolysis to form silica, which also helps to passivate the PNCs.[26,31,48]

The form of existence of amino acids depends on the pH of the solution. When the pH of the solution is greater than the isoelectric point of the amino acid, the amino acid is electronegative; otherwise, the amino acid is electropositive. Using the K_a, K_b, and K_{eq} values and the initial reactant concentrations of OA and APTES, we can calculate the concentration of H^+ produced from their reaction (see the Supporting Information). The concentration of H^+ is 0.60 mM, and the corresponding pH of the solution is 3.22. When Phe is used in combination with OA and APTES, it mainly exists in the form of $H_2N{-}C_8H_8{-}COO^-$, which helps to passivate the PNCs by binding with $CH_3NH_3^+$ and Pb^{2+} through ionic bonding. Since there are lone pair electrons on the N atom in the $-NH_2$ group, Phe can also passivate the PNC surface defects by coordinating with Pb^{2+} or $CH_3NH_3^+$. According to a previous study, the delocalized π bonding system makes the benzene ring a possible electron donor, which could interact with electron acceptors.[59] Thus, it is possible that the benzene ring on Phe could also interact with the uncoordinated Pb^{2+} through π electrons. Therefore, the combined use of Phe, OA, and APTES enables the passivation of the perovskite surface defects more effectively.

In the MPAA-PNC system, based on the proton transfer reaction between MPA and APTES (see the Supporting Information), passivation is achieved mainly through the strong interactions between deprotonated MPA ($-PO_3^{2-}$ and $-PO_3H^-$) and $CH_3NH_3^+$ or Pb^{2+} defects or between protonated APTES ($-NH_3^+$) and Br^- defects.[23] The pH of the solution can also be calculated using the acid dissociation constants, base dissociation constant, and the initial reactant concentrations of MPA and APTES (see the Supporting Information).[31] The corresponding pH is calculated to be 1.80. When Phe is employed, the dissolved Phe mainly exists in the form of $^+H_3N{-}C_8H_8{-}COOH$, suggesting that Phe can passivate the surface Br^- by the ammonium end group through ionic bonding. Due to the lone pair electrons on the O atom in the $-COOH$ group, Phe can also passivate the PNC surface defects by coordinating with Pb^{2+} or $CH_3NH_3^+$, but this effect may be relatively less important.

The ligand binding modes of ligands on the surface of PNCs are summarized in Figure 7 to illustrate the passivation mechanisms. In comparison, the multiligand approach with OA (or MPA), APTES, and Phe leads to the best passivation results in terms of both stability and PL QY. This is attributed to the multiple ions and functional groups from the multiple ligands that can most effectively passivate the various defects on the surface of the PNCs resulting from the constituent ions.

Specifically, for OAA-Phe-PNCs, the passivation is achieved mainly through three possible mechanisms. The first is ionic bonding or interaction between $-COO^-$ anions from OA or Phe and cationic defects ($CH_3NH_3^+$ or Pb^{2+}), as well as between $-NH_3^+$ from APTES and anionic defects (Br^-). The second is coordination between long pair electrons on N in the $-NH_2$ groups in the Phe ligand and cationic defects (Pb^{2+} or $CH_3NH_3^+$). The third is electrostatic interaction between the benzene ring and the uncoordinated Pb^{2+}, which is likely a minor contribution.

In the case of MPAA-Phe-PNCs, the passivation is also achieved mainly through three possible mechanisms. The first is ionic bonding between anionic ligand groups such as $-PO_3^{2-}$ and $-PO_3H^-$ from MPA and cationic defects ($CH_3NH_3^+$ or Pb^{2+}) as well as between cationic ligand groups ($-NH_3^+$ due to Phe or APTES) and anionic defects (Br^-). The second is coordination between Pb^{2+} or $CH_3NH_3^+$ and lone pair electrons on the O atom in the $-COOH$ group of Phe. The third is electrostatic interaction between the benzene ring and the uncoordinated Pb^{2+}.

CONCLUSIONS

In summary, we have demonstrated a multiligand approach involving Phe, APTES, and OA or MPA to passivate $MAPbBr_3$ PNCs for improved stability and optical properties. The different acid ligands, OA vs MPA, affect the way Phe exists and thereby its nature and effectiveness of passivation. The multiple defects of PNCs require a combination of different ligands with multiple functional groups for effective passivation. Importantly, Phe with aromatic and hydrophobic benzene ring as well as both amine and carboxylic acid functional groups can uniquely mediate the pH of the solution and hydrophobicity of the PNC surface, both of which are important for effective passivation of the PNCs. The approach developed is general and can be extended to other combination of ligands, with the key requirement that a careful balance of acid–base equilibrium is established to endow ligands with appropriate functional groups containing electron lone pairs or positive or negative charges for passivating charged surface defects.

ASSOCIATED CONTENT

Supporting Information

The Supporting Information is available free of charge at https://pubs.acs.org/doi/10.1021/acs.jpcc.0c11095.

TEM image and particle size distribution histogram of PNCs; summary of spectroscopic results collected from PNCs containing different ligands; tabulation of peaks and assignments of FTIR spectra; stability test data collected from PNCs under different conditions; and reactions between APTES and OA or MPA (PDF)

AUTHOR INFORMATION

Corresponding Author

Jin Z. Zhang – *Department of Chemistry and Biochemistry, University of California, California 95064, United States;* orcid.org/0000-0003-3437-912X; Phone: +1–831–459-3776; Email: zhang@ucsc.edu

Authors

Li Liu – *Research Institute of Agricultural Quality Standards and Testing Technology, Hubei Academy of Agricultural Science, Wuhan 430064, Hubei, P. R. China; Department of Chemistry and Biochemistry, University of California, California 95064, United States; Hubei Key Laboratory of Nutritional Quality and Safety of Agro products, Wuhan 430064, Hubei, P. R. China*

Ke Xu – *Department of Chemistry and Biochemistry, University of California, California 95064, United States;*

https://dx.doi.org/10.1021/acs.jpcc.0c11095
J. Phys. Chem. C 2021, 125, 2793–2801

College of Chemistry and Chemical Engineering, Chongqing University, Chongqing 401331, Sichuan, P. R. China

A' Lester Allen − *Department of Chemistry and Biochemistry, University of California, California 95064, United States*

Xueming Li − *College of Chemistry and Chemical Engineering, Chongqing University, Chongqing 401331, Sichuan, P. R. China*

Hong Xia − *Research Institute of Agricultural Quality Standards and Testing Technology, Hubei Academy of Agricultural Science, Wuhan 430064, Hubei, P. R. China; Hubei Key Laboratory of Nutritional Quality and Safety of Agro products, Wuhan 430064, Hubei, P. R. China*

Lijun Peng − *Research Institute of Agricultural Quality Standards and Testing Technology, Hubei Academy of Agricultural Science, Wuhan 430064, Hubei, P. R. China; Hubei Key Laboratory of Nutritional Quality and Safety of Agro products, Wuhan 430064, Hubei, P. R. China*

Complete contact information is available at: https://pubs.acs.org/10.1021/acs.jpcc.0c11095

Author Contributions

The manuscript was through the contribution of all authors. All authors have approved the final version of the manuscript.

Notes

The authors declare no competing financial interest.

■ ACKNOWLEDGMENTS

This work was supported by the NSF (CHE-1904547). Work at the Molecular Foundry was supported by the Office of Science, Office of Basic Energy Sciences, of the U.S. Department of Energy under Contract No. DE-AC02-05CH11231. The PXRD data in this work were recorded on an instrument supported by the NSF Major Research Instrumentation (MRI) Program under Grant No. 1126845. We thank Jeremy Barnett for his help with the XRD measurement. L.L. is grateful for support from Hubei Academy of Agricultural Science Visiting Scholar Program (Grant No. Q2018034).

■ REFERENCES

(1) Leng, K.; Fu, W.; Liu, Y.; Chhowalla, M.; Loh, K. P. From Bulk to Molecularly Thin Hybrid Perovskites. *Nat. Rev. Mater.* **2020**, *5*, 482−500.

(2) Yu, X.; Tsao, H. N.; Zhang, Z.; Gao, P. Miscellaneous and Perspicacious: Hybrid Halide Perovskite Materials Based Photodetectors and Sensors. *Adv. Optical Mater.* **2020**, *8*, 2001095.

(3) Shamsi, J.; Urban, A. S.; Imran, M.; De Trizio, L.; Manna, L. Metal Halide Perovskite Nanocrystals: Synthesis, Post-Synthesis Modifications, and Their Optical Properties. *Chem. Rev.* **2019**, *119*, 3296−3348.

(4) Liu, Z. Q.; Zhang, Y. Q.; Fan, Y.; Chen, Z. Q.; Tang, Z. B.; Zhao, J. L.; Lv, Y.; Lin, J.; Guo, X. Y.; Zhang, J. H.; et al. Toward Highly Luminescent and Stabilized Silica-Coated Perovskite Quantum Dots through Simply Mixing and Stirring under Room Temperature in Air. *ACS Appl. Mater Inter.* **2017**, *10*, 13053−13061.

(5) Fu, P.; Shan, Q.; Shang, Y.; Song, J.; Zeng, H.; Ning, Z.; Gong, J. Perovskite Nanocrystals: Synthesis, Properties and Applications. *Sci. Bull.* **2017**, *62*, 369−380.

(6) Almeida, G.; Infante, I.; Manna, L. Resurfacing Halide Perovskite Nanocrystals. *Science* **2020**, *364*, 833−834.

(7) Wei, Y.; Cheng, Z.; Lin, J. An Overview on Enhancing the Stability of Lead Halide Perovskite Quantum Dots and Their Applications in Phosphor-Converted Leds. *Chem. Soc. Rev.* **2019**, *48*, 310−350.

(8) Wang, F.; Geng, W.; Zhou, Y.; Fang, H. H.; Tong, C. J.; Loi, M. A.; Liu, L. M.; Zhao, N. Phenylalkylamine Passivation of Organolead Halide Perovskites Enabling High-Efficiency and Air-Stable Photovoltaic Cells. *Adv. Mater.* **2016**, *28*, 9986−9992.

(9) Vickers, E. T.; Graham, T. A.; Chowdhury, A. H.; Bahrami, B.; Dreskin, B. W.; Lindley, S.; Naghadeh, S. B.; Qiao, Q.; Zhang, J. Z. Improving Charge Carrier Delocalization in Perovskite Quantum Dots by Surface Passivation with Conductive Aromatic Ligands. *ACS Energy Lett.* **2018**, *3*, 2931−2939.

(10) Rambabu, D.; Bhattacharyya, S.; Singh, T.; M, L. C.; Maji, T. K. Stabilization of $MAPbBr_3$ Perovskite Quantum Dots on Perovskite Mofs by a One-Step Mechanochemical Synthesis. *Inorg. Chem.* **2020**, *59*, 1436−1443.

(11) Liu, K. K.; Liu, Q.; Yang, D. W.; Liang, Y. C.; Sui, L. Z.; Wei, J. Y.; Xue, G. W.; Zhao, W. B.; Wu, X. Y.; Dong, L.; et al. Water-Induced $MAPbBr_3$@PbBr(OH) with Enhanced Luminescence and Stability. *Light Sci. Appl.* **2020**, *9*, 44.

(12) Liu, M.; Matuhina, A.; Zhang, H.; Vivo, P. Advances in the Stability of Halide Perovskite Nanocrystals. *Materials* **2019**, *12*, 3733.

(13) Huang, H.; Bodnarchuk, M. I.; Kershaw, S. V.; Kovalenko, M. V.; Rogach, A. L. Lead Halide Perovskite Nanocrystals in the Research Spotlight: Stability and Defect Tolerance. *ACS Energy Lett.* **2017**, *2*, 2071−2083.

(14) Shwetharani, R.; Nayak, V.; Jyothi, M. S.; Geetha Balakrishna, R. Review on Recent Advances of Core-Shell Structured Lead Halide Perovskites Quantum Dots. *J. Alloy. Compd.* **2020**, *834*, 155246.

(15) Luo, B.; Naghadeh, S. B.; Zhang, J. Z. Lead Halide Perovskite Nanocrystals: Stability, Surface Passivation, and Structural Control. *Chem. Nano Mat.* **2017**, *3*, 456−465.

(16) Park, S. M.; Abtahi, A.; Boehm, A. M.; Graham, K. R. Surface Ligands for Methylammonium Lead Iodide Films: Surface Coverage, Energetics, and Photovoltaic Performance. *ACS Energy Lett.* **2020**, *5*, 799−806.

(17) Quarta, D.; Imran, M.; Capodilupo, A. L.; Petralanda, U.; van Beek, B.; De Angelis, F.; Manna, L.; Infante, I.; De Trizio, L.; Giansante, C. Stable Ligand Coordination at the Surface of Colloidal $CsPbBr_3$ Nanocrystals. *J. Phys. Chem. Lett.* **2019**, *10*, 3715−3726.

(18) Zhou, H.; Wang, J.; Wang, M.; Lin, S. Competing Dissolution Pathways and Ligand Passivation-Enhanced Interfacial Stability of Hybrid Perovskites with Liquid Water. *ACS Appl. Mater. Iinter.* **2020**, *12*, 23584−23594.

(19) Pan, A.; He, B.; Fan, X.; Liu, Z.; Urban, J. J.; Alivisatos, A. P.; He, L.; Liu, Y. Insight into the Ligand-Mediated Synthesis of Colloidal $CsPbBr_3$ Perovskite Nanocrystals: The Role of Organic Acid, Base, and Cesium Precursors. *ACS Nano* **2016**, *10*, 7943−7954.

(20) Udayabhaskararao, T.; Houben, L.; Cohen, H.; Menahem, M.; Pinkas, I.; Avram, L.; Wolf, T.; Teitelboim, A.; Leskes, M.; Yaffe, O.; et al. A Mechanistic Study of Phase Transformation in Perovskite Nanocrystals Driven by Ligand Passivation. *Chem. Mater.* **2017**, *30*, 84−93.

(21) Veldhuis, S. A.; Tay, Y. K. E.; Bruno, A.; Dintakurti, S. S. H.; Bhaumik, S.; Muduli, S. K.; Li, M.; Mathews, N.; Sum, T. C.; Mhaisalkar, S. G. Benzyl Alcohol-Treated $CH_3NH_3PbBr_3$ Nanocrystals Exhibiting High Luminescence, Stability, and Ultralow Amplified Spontaneous Emission Thresholds. *Nano Lett.* **2017**, *17*, 7424−7432.

(22) Liu, B.; Li, J.; Duan, G.; Ji, M.; Lu, Y.; Yan, T.; Cao, B.; Liu, Z. Study on Organic-Inorganic Hybrid Perovskite Nanocrystals with Regular Morphologies and Their Effect on Photoluminescence Properties. *Opt. Express* **2020**, *28*, 10714−10724.

(23) Tan, Y. S.; Zou, Y. T.; Wu, L. Z.; Huang, Q.; Yang, D.; Chen, M.; Ban, M. Y.; Wu, C.; Wu, T.; Bai, S.; et al. Highly Luminescent and Stable Perovskite Nanocrystals with Octylphosphonic Acid as a Ligand for Efficient Light-Emitting Diodes. *ACS Appl. Mater Inter.* **2018**, *10*, 3784−3792.

(24) Yang, D.; Li, X.; Zeng, H. Surface Chemistry of All Inorganic Halide Perovskite Nanocrystals: Passivation Mechanism and Stability. *Adv. Mater. Interfaces* **2018**, *5*, 1701662.

(25) Zhang, T. T.; Cao, Z. Q.; Shang, Y. Q.; Cui, C.; Fu, P. F.; Jiang, X. Y.; Wang, F.; Xu, K. M.; Yin, D. G.; Qu, D. H.; et al. Multi-

Functional Organic Molecules for Surface Passivation of Perovskite. *J. Photoch. Photobio. A* **2018**, *355*, 42−47.
(26) Luo, B.; Pu, Y. C.; Lindley, S. A.; Yang, Y.; Lu, L.; Li, Y.; Li, X.; Zhang, J. Z. Organolead Halide Perovskite Nanocrystals: Branched Capping Ligands Control Crystal Size and Stability. *Angew. Chem., Int. Ed.* **2016**, *55*, 8864−8868.
(27) Wang, S.; Huang, F.; Zhou, L.; Wei, J.; Xin, Y.; Jin, P.; Cai, Z.; Yin, Z.; Pang, Q.; Zhang, J. Z. Enhanced Photoluminescence and Stability of $CH_3NH_3PbBr_3$ Perovskite Nanocrystals with Protonated Melamine. *Chem. Nano Mat.* **2018**, *4*, 409−416.
(28) Wang, Y.; Luo, L.; Chen, L.; Ng, P. F.; Lee, K. I.; Fei, B. Enhancement of Stability and Photocatalytic Performance on Hybrid Perovskite with Aniline. *Chem. Nano Mat.* **2018**, *4*, 1054−1058.
(29) Wei, J.; Huang, F.; Wang, S.; Zhou, L.; Jin, P.; Xin, Y.; Cai, Z.; Yin, Z.; Pang, Q.; Zhang, J. Z. Highly Stable Hybrid Perovskite Solar Cells Modified with Polyethylenimine Via Ionic Bonding. *Chem. Nano Mat.* **2018**, *4*, 649−655.
(30) Wei, Y.; Deng, X.; Xie, Z.; Cai, X.; Liang, S.; Ma, P. A.; Hou, Z.; Cheng, Z.; Lin, J. Enhancing the Stability of Perovskite Quantum Dots by Encapsulation in Crosslinked Polystyrene Beads Via a Swelling-Shrinking Strategy toward Superior Water Resistance. *Adv. Funct. Mater.* **2017**, *27*, 1703535.
(31) Xu, K.; Vickers, E. T.; Rao, L.; Lindley, S. A.; Allen, A. C.; Luo, B.; Li, X.; Zhang, J. Z. Synergistic Surface Passivation of $CH_3NH_3PbBr_3$ Perovskite Quantum Dots with Phosphonic Acid and (3-Aminopropyl)Triethoxysilane. *Chem. − Eur. J.* **2019**, *25*, 5014−5021.
(32) Zhang, H.; Nazeeruddin, M. K.; Choy, W. C. H. Perovskite Photovoltaics: The Significant Role of Ligands in Film Formation, Passivation, and Stability. *Adv. Mater.* **2019**, *31*, 1805702.
(33) Zhang, J. Z. A "Cocktail" Approach to Effective Surface Passivation of Multiple Surface Defects of Metal Halide Perovskites Using a Combination of Ligands. *J. Phys. Chem. Lett.* **2019**, *10*, 5055−5063.
(34) Du, J.; Feng, L.; Guo, X.; Huang, X.; Lin, Z.; Su, J.; Hu, Z.; Zhang, J.; Chang, J.; Hao, Y. Enhanced Efficiency and Stability of Planar Perovskite Solar Cells by Introducing Amino Acid to SnO_2/Perovskite Interface. *J. Power Sources* **2020**, *455*, 227974.
(35) Yun, S. C.; Ma, S.; Kwon, H. C.; Kim, K.; Jang, G.; Yang, H.; Moon, J. Amino Acid Salt-Driven Planar Hybrid Perovskite Solar Cells with Enhanced Humidity Stability. *Nano Energy* **2019**, *59*, 481−491.
(36) Zhao, J.; Cao, S.; Li, Z.; Ma, N. Amino Acid-Mediated Synthesis of $CsPbBr_3$ Perovskite Nanoplatelets with Tunable Thickness and Optical Properties. *Chem. Mater.* **2018**, *30*, 6737−6743.
(37) Luo, B.; Naghadeh, S. B.; Allen, A. L.; Li, X.; Zhang, J. Z. Peptide-Passivated Lead Halide Perovskite Nanocrystals Based on Synergistic Effect between Amino and Carboxylic Functional Groups. *Adv. Funct. Mater.* **2017**, *27*, 1604018.
(38) Jancik Prochazkova, A.; Demchyshyn, S.; Yumusak, C.; Másilko, J.; Brüggemann, O.; Weiter, M.; Kaltenbrunner, M.; Serdar Sariciftci, N.; Krajcovic, J.; Salinas, Y.; et al. Proteinogenic Amino Acid Assisted Preparation of Highly Luminescent Hybrid Perovskite Nanoparticles. *ACS Appl. Nano Mater.* **2019**, *2*, 4267−4274.
(39) Sharma, A. K.; Bansal, P.; Nim, G. K.; Kar, P. Essential Amino Acid−Enabled Lead Bromide Perovskite Nanocrystals with High Stability. *Part. Part. Syst. Charact.* **2019**, *36*, 1900328.
(40) Shih, Y. C.; Lan, Y. B.; Li, C. S.; Hsieh, H. C.; Wang, L.; Wu, C. I.; Lin, K. F. Amino-Acid-Induced Preferential Orientation of Perovskite Crystals for Enhancing Interfacial Charge Transfer and Photovoltaic Performance. *Small* **2017**, *13*, 1604305.
(41) Wang, S. N.; Zhou, L. Y.; Huang, F. R.; Xin, Y. L.; Jin, P.; Ma, Q. X.; Pang, Q.; Chen, Y. B.; Zhang, J. Z. Hybrid Organic−Inorganic Lead Bromide Perovskite Supercrystals Self-Assembled with L-Cysteine and Their Good Luminescence Properties. *J. Mater. Chem. C* **2018**, *6*, 10994−11001.
(42) Jancik Prochazkova, A.; Salinas, Y.; Yumusak, C.; Bruggemann, O.; Weiter, M.; Sariciftci, N. S.; Krajcovic, J.; Kovalenko, A. Cyclic Peptide Stabilized Lead Halide Perovskite Nanoparticles. *Sci. Rep.* **2019**, *9*, 12966.
(43) Zhang, W.; Lei, X.; Liu, J.; Dong, J.; Yan, X.; Gao, W.; Dong, H.; Ran, C.; Wu, Z. Efficient Charge Collection Promoted by Interface Passivation Using Amino Acid toward High Performance Perovskite Solar Cells. *Phys. Status Solidi RRL* **2019**, *13*, 1800505.
(44) Zhang, C.; Zhang, S.; Miao, X.; Hu, Y.; Staaden, L.; Jia, G. Rigid Amino Acid as Linker to Enhance the Crystallinity of $CH_3NH_3PbI_3$ particles. *Part. Part. Syst. Charact.* **2017**, *34*, 1600298.
(45) Meggiolaro, D.; Angelis, F. D. First-Principles Modeling of Defects in Lead Halide Perovskites: Best Practices and Open Issues. *ACS Energy Lett.* **2018**, *3*, 2206−2222.
(46) Li, H. S.; Shi, J. J.; Deng, J.; Chen, Z. J.; Li, Y. M.; Zhao, W. Y.; Wu, J. H.; Wu, H. J.; Luo, Y. H.; Li, D. M.; et al. Intermolecular π-π Conjugation Self-Assembly to Stabilize Surface Passivation of Highly Efficient Perovskite Solar Cells. *Adv. Mater.* **2020**, *32*, 1907396.
(47) Liu, G.; Zheng, H.; Zhang, L.; Xu, H.; Xu, S.; Xu, X.; Liang, Z.; Pan, X. Tailoring Multifunctional Passivation Molecules with Halogen Functional Groups for Efficient and Stable Perovskite Photovoltaics. *Chem. Eng. J.* **2021**, *407*, 127204.
(48) Wang, T.; Wei, X.; Zong, Y.; Zhang, S.; Guan, W. An Efficient and Stable Fluorescent Sensor Based on APTES-Functionalized $CsPbBr_3$ Perovskite Quantum Dots for Ultrasensitive Tetracycline Detection in Ethanol. *J. Mater. Chem. C* **2020**, *8*, 12196−12203.
(49) Sarang, S.; Bonabi Naghadeh, S.; Luo, B.; Kumar, P.; Betady, E.; Tung, V.; Scheibner, M.; Zhang, J. Z.; Ghosh, S. Stabilization of the Cubic Crystalline Phase in Organometal Halide Perovskite Quantum Dots Via Surface Energy Manipulation. *J. Phys. Chem. Lett.* **2017**, *8*, 5378−5384.
(50) Xu, K.; Allen, A. C.; Luo, B.; Vickers, E. T.; Wang, Q.; Hollingsworth, W. R.; Ayzner, A. L.; Li, X.; Zhang, J. Z. Tuning from Quantum Dots to Magic Sized Clusters of $CsPbBr_3$ Using Novel Planar Ligands Based on the Trivalent Nitrate Coordination Complex. *J. Phys. Chem. Lett.* **2019**, *10*, 4409−4416.
(51) Jia, D.; Chen, J.; Yu, M.; Liu, J.; Johansson, E. M. J.; Hagfeldt, A.; Zhang, X. Dual Passivation of $CsPbI_3$ Perovskite Nanocrystals with Amino Acid Ligands for Efficient Quantum Dot Solar Cells. *Small* **2020**, *16*, 2001772.
(52) Jancik Prochazkova, A.; Gaidies, S.; Yumusak, C.; Brüggemann, O.; Weiter, M.; Sariciftci, N. S.; Scharber, M. C.; Cepe, K.; Zhoril, R.; Krajcovic, J.; et al. Peptide Nucleic Acid Stabilized Perovskite Nanoparticles for Nucleic Acid Sensing. *Mater. Today Chem.* **2020**, *17*, 100272.
(53) Spildo, K.; Blokhus, A. M.; Andersson, A. Surface and Interfacial Properties of Octanoic Acid−Octylamine Mixtures in Isooctane−Water Systems: Influence of Acid: Amine Molar Ratio and Aqueous Phase pH. *J Colloid Interf. Sci.* **2001**, *243*, 483−490.
(54) Vickers, E. T.; Xu, K.; Dreskin, B. W.; Graham, T. A.; Li, X.; Zhang, J. Z. Ligand Dependent Growth and Optical Properties of Hybrid Organo-Metal Halide Perovskite Magic Sized Clusters. *J. Phys. Chem. C* **2019**, *123*, 18746−18752.
(55) Barja, B. C.; Tejedor-Tejedor, M. I.; Anderson, M. A. Complexation of Methylphosphonic Acid with the Surface of Goethite Particles in Aqueous Solution. *Langmuir* **1999**, *15*, 2316−2321.
(56) Kim, Y.; Yassitepe, E.; Voznyy, O.; Comin, R.; Walters, G.; Gong, X.; Kanjanaboos, P.; Nogueira, A. F.; Sargent, E. H. Efficient Luminescence from Perovskite Quantum Dot Solids. *ACS Aappl. Mater. Inter.* **2015**, *7*, 25007−25013.
(57) Aristidou, N.; Sanchez-Molina, I.; Chotchuangchutchaval, T.; Brown, M.; Martinez, L.; Rath, T.; Haque, S. A. The Role of Oxygen in the Degradation of Methylammonium Lead Trihalide Perovskite Photoactive Layers. *Am. Ethnol.* **2015**, *54*, 8326−8330.
(58) Bryant, D.; Aristidou, N.; Pont, S.; Sanchez-Molina, I.; Chotchunangatchaval, T.; Wheeler, S.; Durrant, R. J.; Haque, S. A. Light and Oxygen Induced Degradation Limits the Operational Stability of Methylammonium Lead Triiodide Perovskite Solar Cells. *Energy Environ. Sci.* **2016**, *9*, 1655−1660.

https://dx.doi.org/10.1021/acs.jpcc.0c11095
J. Phys. Chem. C 2021, 125, 2793−2801

(59) Zhuang, J.; Mao, P.; Luan, Y. G.; Yi, X. H.; Tu, Z. Y.; Zhang, Y. Y.; Yi, Y. P.; Wei, Y. Z.; Chen, N. L.; Lin, T.; et al. Interfacial Passivation for Perovskite Solar Cells: The Effects of the Functional Group in Phenethylammonium Iodide. *ACS Energy Lett.* **2019**, *4*, 2913−2921.

https://dx.doi.org/10.1021/acs.jpcc.0c11095
J. Phys. Chem. C 2021, 125, 2793−2801